Journal of Hazardous Materials, 31 (1992) 155–176
Elsevier Science Publishers B.V., Amsterdam

Modelling heavy gas cloud transport in sloping terrain

J. Kukkonen and J. Nikmo

Finnish Meteorological Institute, Air Quality Department, Sahaajankatu 22 E, SF-00810 Helsinki (Finland)

(Received July 7, 1991; accepted in revised form March 9, 1992)

Abstract

A model is presented for the transport of a denser-than-air gas cloud on a slope. We discuss the structure of the model and derive detailed model equations for the special case in which the wind is directly uphill or downhill. The model was designed as a hazard analysis tool, and its computer implementation can be used as a subprogram in heavy gas dispersion models. We have compared model predictions with results of the Thorney Island phase I field experiments. Although these trials were conducted on flat terrain, the comparison is useful for understanding the cloud transport processes. We have also analysed numerical calculations of heavy gas cloud dispersion on a slope.

1. Introduction

Considerable quantities of toxic and flammable gases are commonly used in many kinds of industrial installations. Many hazardous gases are stored and transported in bulk in liquid form, under pressure at atmospheric temperature, or refrigerated at their boiling point. Serious hazard may be caused to the public in the event of accidental releases of these substances.

In many cases of interest a denser-than-air gas cloud will be formed. This may be due to the low temperature of the gas cloud, the high molecular weight of the substance, or both. The atmospheric dispersion of heavy gas clouds is substantially different from the dispersion of trace contaminants, which follow the atmospheric flow passively.

The currently available heavy gas dispersion models are valid for homogeneous or flat terrain only. However, in safety analysis studies the terrain structure is often highly variable. Field and laboratory experiments have demonstrated that the influence of terrain variability and obstacles on heavy gas dispersion may be substantial (for instance, [1,2]). Recently, Brighton et al. [3] have presented a comprehensive review of the empirical evidence of obsta-

Correspondence to: Dr. J. Kukkonen, Finnish Meteorological Institute, Air Quality Department, Sahaajankatu 22 E, SF-00810 Helsinki (Finland).

cle effects in heavy gas dispersion. The influence of obstructions is more pronounced for heavy gas clouds compared to trace contaminants, as the former may be dispersed near ground level over a wide area.

Generally, obstacles and other structures may have either mitigating or aggravating effects. Obstacles and terrain features change the ambient flow field. The presence of buildings causes increased turbulence, which enhances dispersion; on the other hand, the presence of barriers can restrict the spreading process, decreasing the rate of dilution of the gas cloud [3,4].

We address here the transport of a heavier-than-air gas cloud on an inclined plane. In many heavy gas dispersion models the gas cloud is assumed to be transported downwind at the undisturbed ambient wind speed, reduced to a specified height. For instance, the DENZ [5] and CRUNCH [6] models assume a cloud speed equal to the wind velocity at the cloud half-height. Experimental evidence shows that this assumption gives cloud speeds which are too large [7,8].

The most profound modelling approach to the behaviour of clouds on slopes is the shallow-water theory (for instance, [9]). Jones et al. [10] present numerical solutions of the shallow-water equations for instantaneous releases of (non-entraining, two-dimensional) clouds in still air. They also present analytical results, in particular for the limiting motion of a cloud down a slope.

The present authors adopt a simpler procedure; our starting point is the complete equation of motion of the gas cloud. Bradley et al. [11] have modelled heavy gas cloud transport on flat terrain based on this approach. de Nevers [12] has estimated the transport of a heavy gas cloud downhill in calm air. Deaves and Hall [13] have also developed a model for heavy gas cloud transport. However, their model does not include the influence on cloud transport of the buoyancy of the ambient air. Part of our work is based on the above papers.

All of these models address only the one-dimensional case, in which the wind is directly downhill or uphill. We shall first derive model equations for the three-dimensional case, allowing for any wind direction with respect to the slope. Second, detailed model equations are written for the one-dimensional case. The dependency of the drag force on wind shear has been explicitly taken into account in the model. Third, it is shown that under certain simplifying assumptions about this dependency, we can derive analytical solutions to the one-dimensional model equations.

The presently available experimental data is insufficient for validating the model in the presence of a slope. However, useful information on the factors affecting cloud transport was obtained by comparing model predictions with results of the Thorney Island field experiments [14–16]. We have also presented numerical results for selected example cases. For a more detailed account of this study, the reader is referred to a previous report by the present authors [17].

2. The mathematical model

Only instantaneous releases are considered, and the shape of the gas cloud is assumed to be cylindrical. We neglect the influence of the sloping ground on the spreading and dilution of the gas cloud, and discuss only its transport. The plane is assumed to be substantially larger than the dimensions of the gas cloud, i.e. the model does not allow for varying transport velocities in different parts of the gas cloud.

The wind profile on the inclined plane is generally different from the wind profile on level ground. However, the model equations can be written in a general form, irrespective of the form of the modified wind profile.

To obtain numerical results, the transport model presented has to be incorporated into a heavy gas dispersion program. The derivation of the model equations is nevertheless possible without reference to any specific dispersion model.

2.1 Equation of motion of the gas cloud

Figure 1 shows the forces acting on an instantaneously released heavy gas cloud on an inclined plane. D is the aerodynamic drag due to the ambient wind flow, F is the friction force between the cloud and ground, and F_{g-b} is the gravity minus buoyancy force (the support of the ground is neglected in the figure).

The x and y-axes are parallel to the inclined plane and the z-axis is perpendicular to it. The x-axis is in the uphill direction. We denote by $\bar{\mathbf{u}}(z')$ the undisturbed wind profile far from the slope, and by $\bar{\mathbf{u}}_s(z)$ the wind profile on the slope. The inclination angle of the inclined plane is θ and its orientation angle with respect to the wind vector is ϕ. The inclination angle ranges from 0° to 90° and the orientation angle from 0° to 360°.

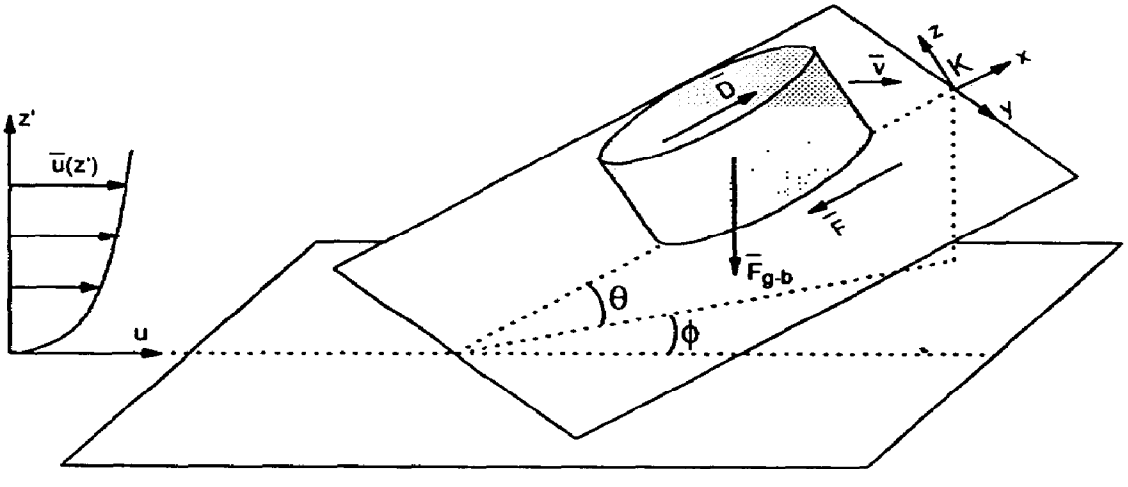

Fig. 1. A schematic figure of an instantaneously released heavy gas cloud on an inclined plane.

The equation of motion of the gas cloud can be written in the vector form:

$$\frac{\mathrm{d}}{\mathrm{d}t}[m_c\bar{v}] = \frac{\mathrm{d}}{\mathrm{d}t}[(m_e + m_t + m_g)\bar{v}] = \bar{D} + \bar{F} + \bar{F}_{g-b} + \dot{m}_e\bar{u}_{s,av} + \dot{m}_t\bar{u}_s(h) \quad (1)$$

where $\bar{v}$ is the velocity of the cloud, m_c is the total mass of the cloud, m_e and m_t are the masses of entrained air through the cloud edge and top surfaces, respectively, and m_g is the mass of the released gas. Deposition is neglected in eq. (1), and therefore the mass of the released gas is constant.

The right-hand side of eq. (1) also includes the change of momentum due to air entrainment at the edge and top surfaces of the cloud. $\bar{u}_{s,av}$ is the average wind velocity at the edge surface of the gas cloud. Its computation will be discussed later. $\bar{u}_s(h)$ is the wind velocity at the height of the gas cloud, h. In the following we shall discuss the modelling of the forces $\bar{D}$, $\bar{F}$ and $\bar{F}_{g-b}$.

For a cylindrical gas cloud, allowing for the wind shear, the drag force can be written in the form

$$\bar{D} = \int_0^h C(Re)R\delta_a|\bar{U}(z)|\bar{U}(z)\,\mathrm{d}z \quad \text{where } \bar{U}(z) = \bar{u}_s(z) - \bar{v} \quad (2)$$

where $C(Re)$ is the drag coefficient, R is the radius of the cloud, δ_a is the density of the ambient air and $\bar{U}$ is the velocity of the ambient flow with respect to the velocity of the cloud. The drag coefficient is a function of the shape of the body and the Reynolds number, Re.

The application of eq. (2) requires that the gas cloud is sufficiently coherent with respect to the ambient flow field. This should be a reasonable assumption for gas clouds which are substantially heavier than ambient air. Further, experimental data for drag coefficients have been determined for a homogeneous flow field, with the object submerged in the flow. For releases into the atmosphere near ground level, the flow profile is logarithmic and the ground prevents flow on one side of the gas cloud. Some inaccuracy is therefore to be expected in applying these results for heavy gas dispersion.

The measured drag coefficient of a circular cylinder normal to the stream as a function of Re ranges from about 0.3 to 1.2, in the regime $Re = 10^5 - 10^7$ [18]. These results are valid for large aspect ratios h/d (h is the height and d is the diameter of the cylinder). Hughes and Brighton [19] have presented drag coefficients for a circular cylinder normal to the stream, in the regime $10^3 < Re < 10^5$, for different aspect ratios. For instance, $C = 0.63$ for $h/d = 1$, and $C = 1.2$ for $h/d \to \infty$.

The Reynolds number for a gas cloud can be defined as $Re = \delta_a uL/\mu$, where L is a characteristic length of the body ($L = 2R$), u is the velocity of the ambient flow with respect to the gas cloud ($u = u_s(z) - v$) and μ is the dynamic viscosity of air. Numerical computations with the present model for the gas clouds of

the Thorney Island experiments show that the Reynolds numbers range from approximately 10^5 to 10^7. The initial aspect ratio h/d in the experiments was about 1.0, and the computed minimum values of the aspect ratio were typically a few per cent.

We conclude that the drag coefficient ranges from about 0.5 to 1.0. In the numerical computations, we used the value $C=0.5$, which is valid in the highly turbulent region, for gas clouds having a small aspect ratio. Bradley et al. [11] and de Nevers [12] in their computations have used the value $C=1.0$. The sensitivity of the model results to C is discussed later.

The friction force between the gas cloud and the ground can be written in the form [11]

$$F=\tau\pi R^2=\delta_c\left[\frac{u_*}{u(10)}\right]^2 v^2\pi R^2 \tag{3}$$

where τ is the turbulent shear stress, δ_c is the density of the cloud, u_* is the friction velocity and $u(10)$ is the wind velocity at 10 m height. As the direction of the friction force $\bar{F}$ is opposite to the direction of the velocity of the gas cloud, $F_x=Fv_x/v$ and $F_y=Fv_y/v$.

The gravity minus buoyant force acting on the cloud is given by

$$F_{g-b}=\pi R^2 h\delta_a\left[\frac{\delta_c-\delta_a}{\delta_a}\right]g=\pi R^2 h\delta_a g' \tag{4}$$

where $g'=g(\delta_c-\delta_a)/\delta_a$ is the reduced acceleration of gravity.

As the mass of the released gas is constant, $\dot{m}_g$ $(=\mathrm{d}m_g/\mathrm{d}t)=0$. Expanding eq. (1) in scalar form yields

$$m_c\dot{v}_x=D_x-F_x+\dot{m}_e[\bar{u}_{s,av}\cdot\hat{e}_x-v_x]+\dot{m}_t[\bar{u}_s(h)\cdot\hat{e}_x-v_x]-F_{g-b}\sin\theta \tag{5a}$$

and

$$m_c\dot{v}_y=D_y-F_y+\dot{m}_e[\bar{u}_{s,av}\cdot\hat{e}_y-v_y]+\dot{m}_t[\bar{u}_s(h)\cdot\hat{e}_y-v_y] \tag{5b}$$

where $\hat{e}_x$ and $\hat{e}_y$ are the unit vectors in the x and y-directions, and the signs of the different terms have been chosen according to the notation in Fig. 1. $\dot{m}_e$ and $\dot{m}_t$ are the rates of air entrainment at the cloud edge and cloud top surfaces, respectively. If the wind profile on the slope $\bar{u}_s(z)$ is known, the velocity of the gas cloud $(\bar{v})$ can be solved numerically from eqs. (5a,b), with the forces given in eqs. (2)–(4).

For sufficiently small slope inclination angles, the influence of slope on the direction of the wind is negligible. Neglecting also the influence of the gas cloud on the wind field, one obtains

$$\bar{u}_{s,av}\cdot\hat{e}_x=u_{s,av}\cos\phi \tag{6a}$$

$$\bar{u}_s(h)\cdot\hat{e}_x=u_s(h)\cos\phi \tag{6b}$$

$$\bar{\boldsymbol{u}}_{s,av}\cdot\hat{\boldsymbol{e}}_y = u_{s,av}\sin\phi \tag{6c}$$

and

$$\bar{\boldsymbol{u}}_s(h)\cdot\hat{\boldsymbol{e}}_y = u_s(h)\sin\phi \tag{6d}$$

Equations (5a,b) reduce to a simpler form with the help of these relations.

2.2 The one-dimensional case

The above model is applicable for any direction of the wind with respect to the slope. In the following we shall derive model equations for the case in which the wind is directly uphill or downhill. The orientation angle of the inclined plane ϕ is therefore taken to be equal to 0° or 180°.

We assume also that the gas cloud is initially moving in the direction of the wind, or opposite to that direction. Under these assumptions the gas cloud is transported along the x-axis. For simplicity, we shall omit the subscript x in this chapter (denoting v_x with v, F_x with F and D_x with D). We shall also denote $u_{s,av}$ with u_{av} and $u_s(h)$ with $u(h)$.

Equations 5(a) and (b) reduce to a one-dimensional form

$$m_c\dot{v} = D - F + \dot{m}_e[u_{av}\cos\phi - v] + \dot{m}_t[u(h)\cos\phi - v] - F_{g-b}\sin\theta \tag{7}$$

Neglecting the dependence of the drag coefficient on height, the drag force eq. (2) reduces to

$$D = CR\delta_a\int_0^h [u(z)-v]\,|u(z)-v|\,dz \tag{8}$$

We use a simple logarithmic wind profile

$$u(z) = \frac{u_*}{k}\ln\left[\frac{z}{z_0}\right] \tag{9}$$

where z_0 is the roughness length and k is Von Karman's constant. The zero-plane displacement of the wind profile and the correction factors due to atmospheric stability have been neglected in eq. (9) (for instance, [20]). By definition, $u(z)=0$ when $z \le z_0$.

2.2.1 Computation of the drag force

The expression for the drag force (8) can be integrated analytically. The form of the solution depends on the initial value of the cloud speed. As an example, we shall consider the case when the initial cloud velocity v is positive and its value is less than the wind speed at the top of the cloud, $u(h)$.

The cloud speed and the wind speed are equal at some height, i.e. $u(h_0)=v$. Using eq. (9) yields $h_0 = z_0\exp(kv/u_*)$. The drag force integral (8) can now be separated into three terms

$$D=CR\delta_a\left[-\int_0^{z_0} v^2\mathrm{d}z-\int_{z_0}^{h_0}[u(z)-v]^2\mathrm{d}z+\int_{h_0}^{h}[u(z)-v]^2\mathrm{d}z\right] \tag{10}$$

This equation has a clear physical interpretation. Up to the height h_0, the wind velocity is smaller than the velocity of the cloud, and the first and second terms on the right-hand side of eq. (10) therefore correspond to resisting (negative) forces. Above height h_0, the wind velocity is larger than the velocity of the cloud, and therefore the third term corresponds to a driving (positive) force.

Using the wind profile (9), the integrals in eq. (10) can be solved in closed form. The integration can also be performed for cases in which the initial cloud velocity is larger than the wind velocity at the top of the cloud, and when the initial cloud velocity is negative [17].

2.2.2 Equation of motion

The average wind speed over the cloud height u_{av} is needed for the computation of momentum entrained from the edge surface of the gas cloud. The average wind speed is, by definition,

$$u_{av}=\frac{1}{h}\int_0^h u(z)\mathrm{d}z$$

which yields

$$u_{av}=u(h)-\frac{u_*}{k}\left[1-\frac{z_0}{h}\right] \tag{11}$$

Clearly, as $h>z_0$, $u_{av}<u(h)$.

The equation of motion (7) can now be written in a form which is better suited for numerical computations, using the integrated form of the drag force and eqs. (3), (4), (9) and (11). A straightforward but lengthy computation gives as the final result

$$m_c\dot{v}=\alpha v^2+\beta v-\sigma\exp(kv/u_*)+\epsilon-B \tag{12}$$

Equation (12) has been written in terms of the descending powers of v. The factor B is given by

$$B=\pi R^2 h\delta_a\left[\frac{\delta_c-\delta_a}{\delta_a}\right]g\sin\theta \tag{13}$$

The form of factors α, β, σ and ϵ is dependent on the value of the cloud speed:

(i) The solution for $0\le v\le u(h)$.

$$\alpha=[C\delta_a h-\delta_c[u_*/u(10)]^2\pi R]R \tag{14a}$$

$$\beta = 2CR\delta_a[u_*(h+z_0)/k - hu(h)] - \dot{m}_e - \dot{m}_t \quad (14b)$$

$$\sigma = 4z_0 CR\delta_a(u_*/k)^2 \quad (14c)$$

and

$$\epsilon = u(h)[CR\delta_a h[u(h) - 2u_*/k] + (\dot{m}_e + \dot{m}_t)\cos\phi] + 2CR\delta_a(u_*/k)^2(h+z_0) - \dot{m}_e(u_*/k)(1 - z_0/h)\cos\phi \quad (14d)$$

(ii) The solution for $v > u(h)$.

$$\alpha = [-C\delta_a h - \delta_c[u_*/u(10)]^2\pi R]R \quad (15a)$$

$$\beta = 2CR\delta_a[u_*(z_0 - h)/k + hu(h)] - \dot{m}_e - \dot{m}_t \quad (15b)$$

$$\sigma = 0 \quad (15c)$$

and

$$\epsilon = -u(h)[CR\delta_a h[u(h) - 2u_*/k] - (\dot{m}_e + \dot{m}_t)\cos\phi] - 2CR\delta_a(u_*/k)^2(h - z_0) - \dot{m}_e(u_*/k)(1 - z_0/h)\cos\phi \quad (15d)$$

(iii) The solution for $v < 0$.

$$\alpha = [C\delta_a(h - 2z_0) - \delta_c[u_*/u(10)]^2\pi R]R \quad (16a)$$

$$\beta = 2CR\delta_a[u_*(h - z_0)/k - hu(h)] - \dot{m}_e - \dot{m}_t \quad (16b)$$

$$\sigma = 0 \quad (16c)$$

and

$$\epsilon = u(h)[CR\delta_a h[u(h) - 2u_*/k] + (\dot{m}_e + \dot{m}_t)\cos\phi] + 2CR\delta_a(u_*/k)^2(h - z_0) - \dot{m}_e(u_*/k)(1 - z_0/h)\cos\phi \quad (16d)$$

The velocity of the gas cloud can now be solved from the differential equation (12), where the various terms have been defined in eqs. (13)–(16). It can be shown that the resulting solution of v is continuous, i.e. solutions (i) and (ii) yield equal results at $v = u(h)$, and (i) and (iii) yield equal results at $v = 0$. In the numerical model, the solution appropriate for each grid intervals has been used.

2.2.3 A simplified model

A simplified form of the drag force and the equation of motion can be derived making the approximation

$$D \approx CR\delta_a(u_{av} - v)^2 h \quad (17)$$

Clearly, this approximation always produces a positive drag force, while the more general equation (10) allows for both the resisting (negative) and driving (positive) forces. The limits of validity of eq. (17) are therefore more strict, compared to eq. (10).

Using eq. (17) yields the following differential equation for the velocity of the gas cloud (the derivation is similar to the previous computations):

$$m_c\dot{v} = \Gamma v^2 - \Omega v + \Sigma - B \tag{18}$$

where

$$\Gamma = [C\delta_a h - \delta_c [u_*/u(10)]^2 \pi R] R \tag{19a}$$

$$\Omega = 2CR\delta_a h[u(h) - (u_*/k)(1 - z_0/h)] + \dot{m}_e + \dot{m}_t \tag{19b}$$

and

$$\Sigma = CR\delta_a h[u(h) - (u_*/k)(1 - z_0/h)]^2 + \dot{m}_e[u(h) - (u_*/k)(1 - z_0/h)] + \dot{m}_t u(h) \tag{19c}$$

The variables can be separated in the differential equation (18), and the resulting integrals can be solved analytically. The full solution is presented in the following. This solution will later be used to evaluate the accuracy of the simplified model.

We use the following notation:

$$a = \Gamma/m_c, \quad b = -\Omega/m_c, \quad c = (\Sigma - B)/m_c \quad \text{and} \quad K = b^2 - 4ac \tag{20}$$

The form of solution is dependent on the value of K. In the following equations, d_1', d_1'', d_2', d_2'', d_3' and d_3'' are integration constants, determined by the initial velocity and position of the gas cloud.

(i) The case $K < 0$.

$$v(t) = \frac{(-K)^{1/2} \tan[\frac{1}{2}(t + d_1')(-K)^{1/2}] - b}{2a} \tag{21a}$$

$$x(t) = \frac{-\ln|\cos[\frac{1}{2}(-K)^{1/2}(t + d_1')]| - \frac{1}{2}bt}{a} + d_1'' \tag{21b}$$

This solution is given for completeness, but it is actually non-physical ($v(t) \to \infty$ as $t \to \infty$).

(ii) The case $K = 0$.

$$v(t) = -(1/a)[(1/(t + d_2')) + \tfrac{1}{2}b] \tag{22a}$$

$$x(t) = -(1/a)[(\ln|t + d_2'|) + \tfrac{1}{2}bt] + d_2'' \tag{22b}$$

(iii) The case $K>0$.

$$v(t)=\frac{\pm\exp(f(t))(b+K^{1/2})-b+K^{1/2}}{2a[1\mp\exp(f(t))]} \tag{23a}$$

$$x(t)=\frac{-(b+K^{1/2})\ln|1\mp\exp(f(t))|-(K^{1/2}-b)\ln|\exp(-f(t))\mp1|}{2aK^{1/2}}+d_3'' \tag{23b}$$

where the function $f(t)$ has been defined as

$$f(t)=(t+d_3')K^{1/2} \tag{24}$$

We define the variable Φ as follows

$$\Phi=(2av+b-K^{1/2})/(2av+b+K^{1/2}) \tag{25}$$

Equations (23a,b) contain the notations $\mp$ and $\pm$; the upper signs are selected if $\Phi>0$, while the lower signs are selected if $\Phi<0$ ($\Phi=0$ is not possible).

3. Comparison of model predictions with experimental data on level ground

A computer program has been written for solving the gas cloud transport model discussed in the previous chapters. The velocity of the gas cloud is computed from eq. (12), where the various terms have been defined in eqs. (13)–(16a–d). The numerical model was introduced into a modified version of the heavy gas dispersion model DENZ [5]. For details of the numerical procedures and model parameters see our previous report [17].

We have compared model predictions for cloud transport with experimental data from the Thorney Island phase I field experiments [14–16, 21]. These

TABLE 1

Some parameters in the Thorney Island trials selected for the comparison of model and experiments (compiled from [9]). Notation: u=wind speed at 10 m height, T_{amb}=ambient temperature, m_0=mass of the released material, h_0=initial height of the cloud

Trial No.	Pasquill stability class	U (m/s)	T_{amb} (°C)	m_0 (kg)	h_0 (m)
5	B	4.6	22.2	2610	8.6
7	E	3.2	17.1	4260	13.0
8	D	2.4	17.1	3970	13.0
9	F	1.7	18.6	3880	13.0
13	D	7.5	13.2	4810	12.7
19	E	6.4	13.3	5490	13.6

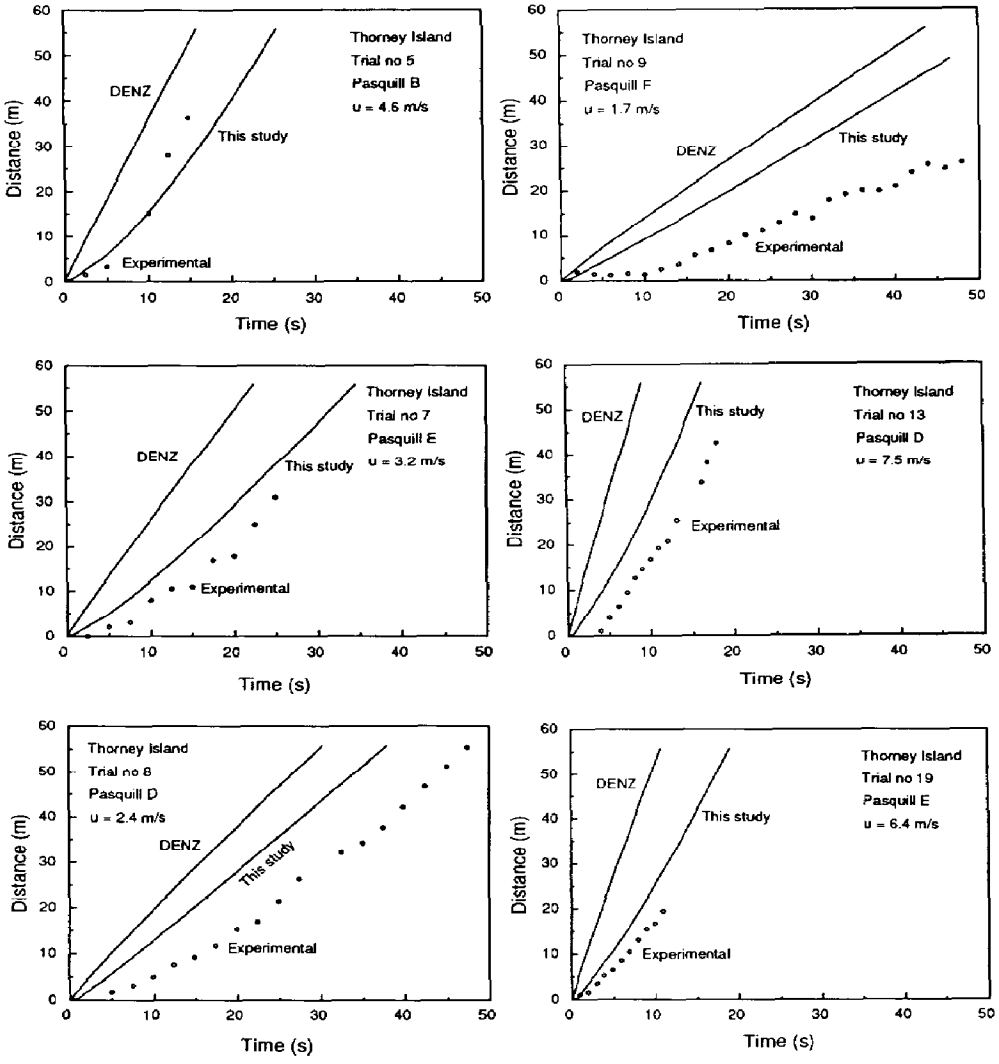

Fig. 2. Experimental results and model predictions on the distance of the cloud centroid from source as a function of time for some Thorney Island trials.

trials were conducted in flat terrain. The presently available experimental data is insufficient for validating the model in the presence of a slope.

Table 1 shows some of the most important parameters in the six trials which we selected for the comparison. Trials No. 7, 8, 9, 13 and 19 were selected because of the good quality of the experimental results and Trial No. 5 was included in order to better cover the range of stability classes. However, in Trial 5 the gas container dropped in two stages and the lid failed to retract [14]. The ground temperatures in the selected trials were assumed to be equal to the ambient temperatures.

Figure 2 shows the results of the comparison. We have computed the solid

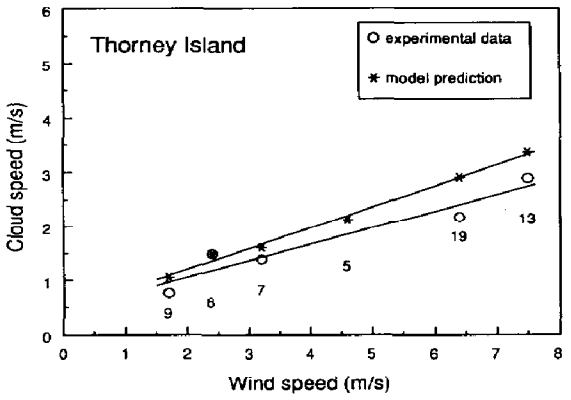

Fig. 3. A compilation of model predictions and experimental data for some Thorney Island field trials. The computed and measured cloud speeds have been shown as a function of the measured wind speed at 10 m height. The trial numbers are also shown in the figure.

curves with the model of the present study and with the model DENZ. The experimental data were taken from Prince et al. [21]. For each trial, the Pasquill class and the wind speed at 10 m height have been indicated.

The predictions of the present model are clearly better compatible with the data, compared to the original DENZ predictions (computed in this work). However, the predicted cloud speeds (dx/dt) are somewhat larger than experimental results for all trials except No. 5.

The experimental results show a delay in the cloud transport at the beginning of each trial, the delay times ranging from about 2 to 10 seconds. This effect may be due to the experimental arrangements, and it is not taken into account in the model computations. A major part of the differences between model results and experiments seems to be caused by this delay.

Prince et al. [21] have made linear regressions of the experimental data for the distance of the cloud centroid against time. The cloud centroid is defined as the centre of mass of the cloud, and its position was determined from still photographs. We have computed the predicted cloud speeds by fitting a line to the predicted distance against time curve for each trial, in the same time interval as in the above study. Clearly, this procedure produces an average cloud speed which is dependent on the specified time interval.

The experimental correlation for Trial No. 5 is based only on three data points, and the cloud speed value is therefore not statistically valid. We shall neglect this data point in the following. These results are summarised in Fig. 3. The straight lines have been drawn as a visual guide only.

The predicted cloud speed values are from 0 to 38% higher than experimental results. The difference is largest for Trials No. 9 and 19. For Trial No. 9, this is due to the substantial delay time of the initial cloud transport (about 10 seconds). For Trial No. 19, the difference may be due to the fact that ex-

perimental data was available only for a short time interval (from 5 to 11 seconds).

4. Numerical results

Numerical computations were made for a moderate release of chlorine (1,000 kg) and a large release of ammonia (40,000 kg). Two kinds of weather conditions were included for the ammonia release (Table 2). The transport of the gas cloud was computed in flat terrain, and for an upslope and a downslope wind on an inclined plane with an inclination angle of 25°.

Initially the substance was assumed to be in liquid form in a pressurized container, at the temperature of the ambient air. We used a simple computer model developed in-house for evaluating the source term of an instantaneous release. This model assumes initial adiabatic depressurisation and subsequent isenthalpic mixing of the two-phase mixture with ambient air.

The amount of entrained air can be specified as input data in the model. We selected the minimum amount of air which is needed to vaporise the liquid phase completely. The cloud is therefore assumed to consist of pure vapour after the source term evolution, and the possible evaporation and spread of liquid on the slope need not then be considered.

The initial cloud speed was assumed to be negligible, and the wind profile on the slope was assumed to be identical to the undisturbed wind profile far from the slope. The roughness length was taken to be 0.10 m.

4.1 The influence of the slope on the cloud speed

Figure 4 shows the influence of an inclined plane on the transport of the gas clouds. Clearly, substantial differences exist between the downslope, upslope and flat terrain cases. For an upslope wind, the gas cloud is first driven down the slope by gravity (the cloud speed is negative), and then forced back up the slope by the wind. For a downslope wind, the cloud speed first increases rapidly

TABLE 2

Accident cases selected for the numerical computations. Notation: T_{amb} = the temperature of the ambient air; wind speed refers to that at 10 m height

Case No.	Released species	Mass of released material (kg)	Meteorological conditions		
			T_{amb} (°C)	Pasquill stability class	Wind speed (m/s)
1	Chlorine	1 000	15	D	4
2	Ammonia	40 000	15	D	4
3	Ammonia	40 000	15	E	2

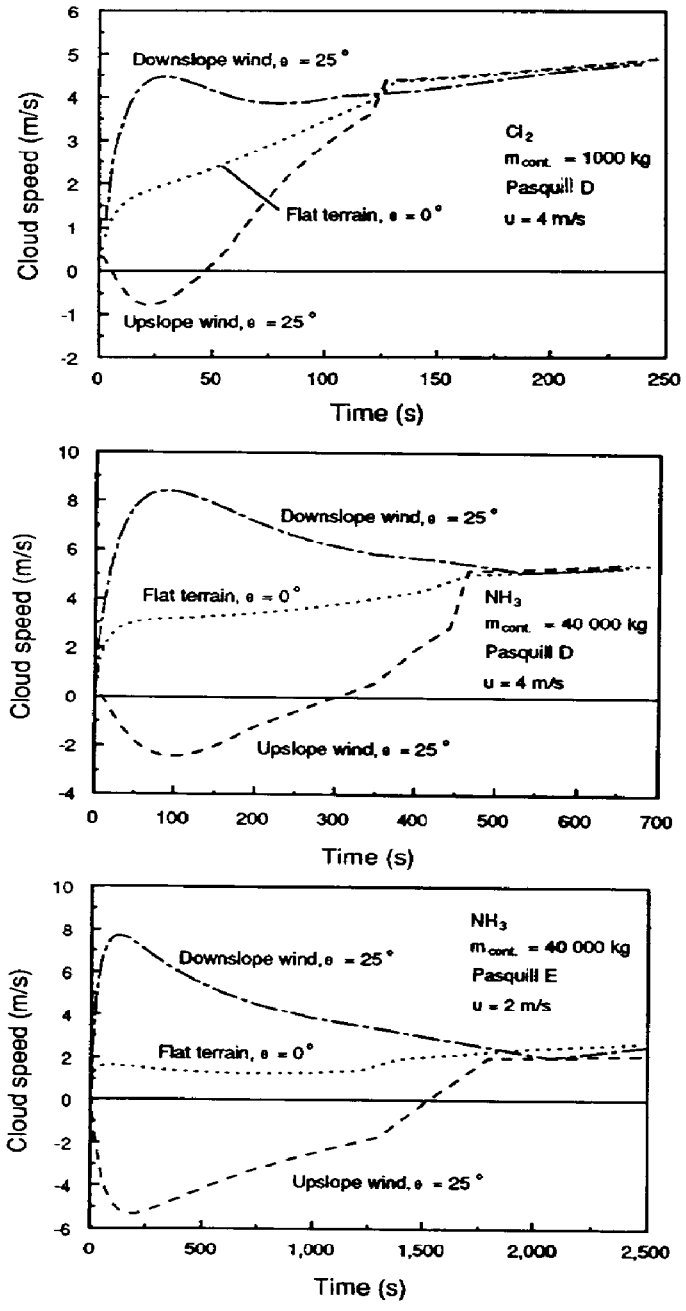

Fig. 4. The speed of the gas cloud as a function of time for the selected accident cases. The results show dispersion in flat terrain and for a downslope and an upslope wind.

due to the combined effect of gravity and the wind, and then decreases slowly due to the decreasing influence of gravity (caused by increasing cloud dilution).

Generally, the influence of the slope is more pronounced for large releases,

for heavy gas clouds, in stable atmospheric conditions and light wind speeds. For instance, the minimum values (for upslope wind) and the maximum values (for downslope wind) of the cloud speed are clearly larger for the large ammonia release compared to the more moderate chlorine release.

The relative significance of all the forces (gravity minus buoyancy, drag and friction) decreases with dilution of the gas cloud and with time. For a sufficiently large dilution, the transport process is governed by the momentum of the entrained air. At sufficiently large distances, the cloud speed curves therefore tend to the same value irrespective of the slope.

4.2 The influence of the slope on the contaminant concentration

Figure 5 shows the variation of the normalised contaminant concentration by mass as a function of the position of the cloud centroid. Positive position values correspond to transport downwind, and negative values transport upwind.

For the upslope wind, the initial transport of the cloud down the slope can be seen for all cases. The distances travelled down the slope are substantially larger for the ammonia release, compared to the chlorine release. The concentrations for the upslope and downslope cases at some fixed position may vary by up to about two orders of magnitude.

Figure 6 shows the same concentration values as Fig. 5, as a function of the distance travelled by the cloud centroid. The concentration values are lowest in an upslope wind for Cases No. 1 and 2, and in flat terrain for Case No. 3. The explanation for this behaviour can be found from Fig. 4, which show that the absolute values of the cloud speed are on average also smallest in the above-mentioned cases. A slowly-moving cloud has more time to disperse, and the concentrations against distance travelled are therefore lower.

We also studied the relative importance of the forces and the momentum entrainment terms on cloud transport (eq. (7)) [17]. For the Thorney Island trials, momentum entrainment and friction against the ground were found to be the most important factors. For a large release on a slope (example cases No. 2 and 3), the gravity minus buoyancy force is the most important term up to substantial downwind distances, and the drag force is also important. For sufficiently large distances, the momentum entrainment terms become dominant for all conceivable releases.

The discontinuities of the first derivative in some of the curves of Figs. 4–6 are due to the inaccuracies of the numerical solution.

4.3 The validity of the simplified model

Three kinds of computational procedures were applied: (1) a numerical solution of the general model, which is based on eqs. (12)–(16a–d); (2) a numerical solution of the simplified model, which is based on eqs. (18) and (19a–c); and (3) the analytical solution of the simplified model, which is based on

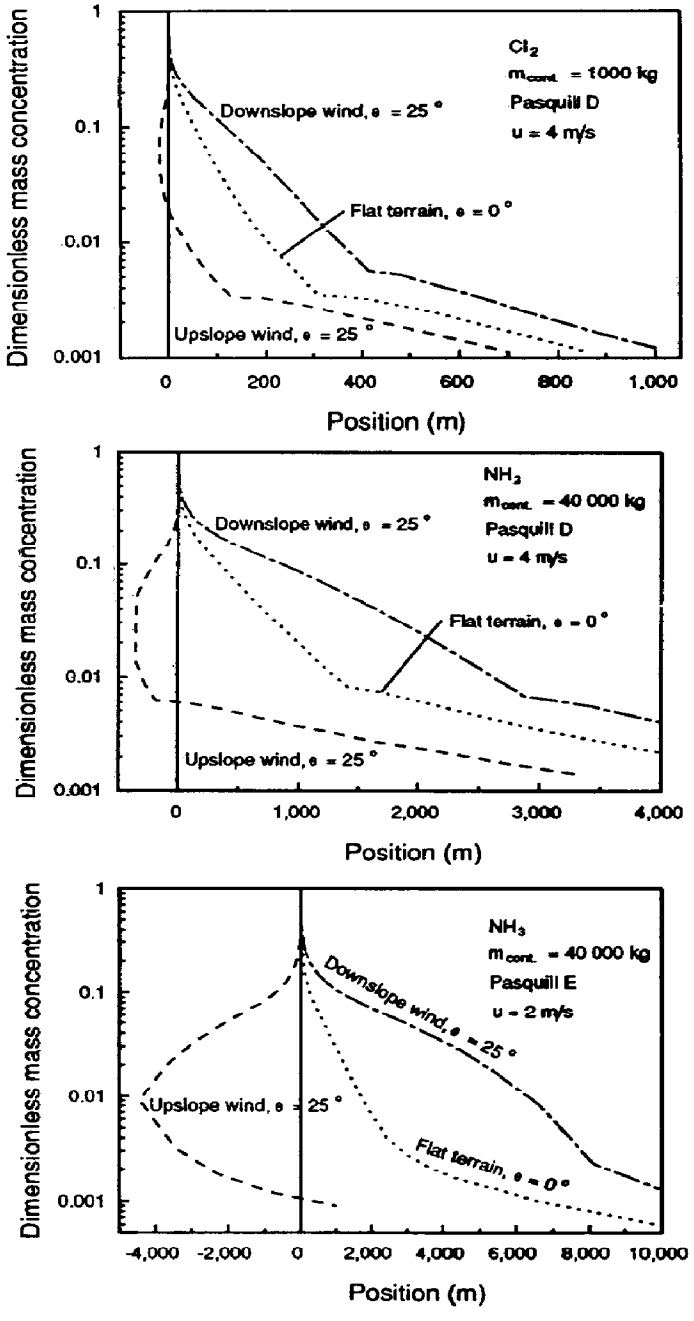

Fig. 5. The dimensionless mass concentration as a function of the position of the gas cloud for the selected accident cases.

eqs. (21a,b)–(23a,b). The numerical solutions (1) and (2) are based on the Runge–Kutta–Merson method [22].

First, to study the accuracy of the adopted numerical procedures, we com-

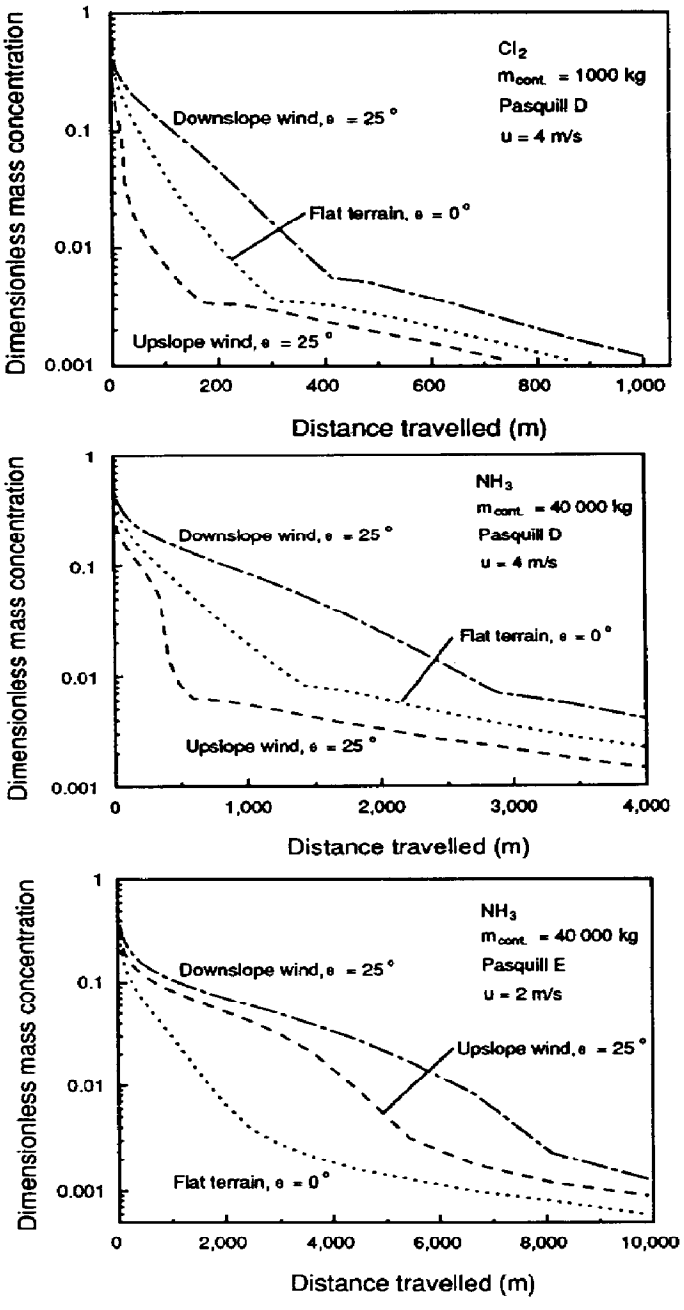

Fig. 6. The dimensionless mass concentration as a function of the distance travelled by the gas cloud for the selected accident cases.

pared the solutions of the simplified model, (2) and (3). The difference in cloud speed computed by these two methods was smaller than 3% in the numerical example cases defined above and for the Thorney Island trials consid-

TABLE 3

The percentage difference in cloud speed predictions, as computed by the general numerical model and by the simplified analytic solution (eqs. (21-23). The dimensionless time is defined as t/t_t, where t_t is the transition time into passive dispersion

Case	Dimensionless time		
	1/4	2/4	3/4
Case 1			
upslope	7	7	1
flat terrain	12	2	1
downslope	24	13	7
Case 2			
upslope	3	10	30
flat terrain	4	2	0
downslope	19	16	8
Case 3			
upslope	0	0	0
flat terrain	1	0	0
downslope	28	15	10

ered. As the numerical schemes in (1) and (2) were identical, this comparison also gives an estimate of the numerical accuracy of the general model.

Second, we studied the limits of validity of the simplified model, by comparing solutions (1) and (3). Table 3 shows the deviation of the analytical solution of the simplified model from the general model, defined as $|v_{(1)}-v_{(3)}|/v_{(1)}$ (%). The differences of the two models were less than or equal to 30% in all the cases considered. The differences are in general larger for the downslope cases, and for small times. The analytical solution tends to overpredict cloud speeds for a downslope wind, as the resisting drag forces are particularly important in that case.

We also studied the sensitivity of the present model on the drag coefficient, using the values $C=0.5$ and $C=1.0$. For the example Case No. 3 in an upslope wind, the cloud speed computed with $C=1.0$ and $C=0.5$ differs for most of the time by 10–20%. The same sensitivity test was also made for the Thorney Island Trial No. 8. The cloud speed values computed using the values $C=0.5$ and 1.0 varied less than 2% [17].

5. Conclusions

A model has been presented for analysing the transport of an instantaneously released heavy gas cloud on a slope. Continuous releases have not been discussed. We have first presented the general model, which allows for an arbitrary wind direction, and then derived the detailed model equations for an

upslope or downslope wind. The computer implementation of the model can be used as a subprogram in heavy gas dispersion models.

It was shown that under certain simplifying assumptions, analytical solutions of the one-dimensional model equations can be derived. The limits of validity of the analytic solution were studied by comparing it to the more general numerical model. In the numerical cases considered, the maximum differences in cloud speed predictions between the two models were about 30%.

The model only addresses the transport processes. Clearly, sloping ground may also have a direct influence on the spreading and dilution of the gas cloud. For instance, the combined effect of wind shear and gravity may change the shape of the gas cloud. The spreading process is also dependent on the direction of the wind with respect to the slope.

The orientation and inclination angles of the plane have been assumed constant. The model equations could also be solved numerically for spatially varying inclinations and orientation angles, i.e. the model could be generalised for more complex geometrical situations. However, this procedure requires that the plane structure does not change too rapidly.

An estimate of the wind profile on the slope is needed to solve the model equations. The evaluation of the ambient flow pattern may be problematic even for fairly simple situations (for instance, [23]). In general, the change of both the wind speed and direction with height are different from the undisturbed wind profile far from the slope.

Model predictions were compared with the results of the Thorney Island field experiments. The predictions of the present model were clearly more compatible with the data, compared to results obtained with simpler assumptions on cloud transport. However, the predicted cloud speeds were in general larger than the experimental results. Most of the difference between the model results and the experiments is caused by a delay in cloud transport at the beginning of each trial. This effect may be due to the experimental arrangements; and it was not possible to take these into account in the computations.

The currently available experimental data is insufficient for validating the model in the presence of a slope. Some experiments on heavy gas cloud dispersion on a slope were conducted in the Porton Down experiments [24], but the results are only qualitative. Britter and Snyder [25] studied dense gas dispersion over a ramp in a wind tunnel, but these results are not directly applicable for validating the present model.

Numerical computations were made for a moderate release of chlorine and a large release of ammonia, in stable and neutral atmospheric stabilities. The transport of gas clouds was analysed in flat terrain, and for an upslope and a downslope wind on a slope with an inclination of 25°.

Substantial differences were found between the downslope, upslope and flat terrain cases. The concentrations for upslope and downslope cases at a fixed position varied by up to about two orders of magnitude. The influence of the

slope is more pronounced for large releases, for heavy gas clouds, in stable atmospheric conditions and light wind speeds.

Numerical results also showed that for upslope wind, the gas cloud may first be driven substantial distances down the slope by gravity, and then forced back up the slope by the wind. The same phenomenon was recorded qualitatively in the Porton Down experiments.

Acknowledgements

The authors wish to thank Mr Esko Ulvelin (Technical Inspection Centre of Finland) and Dr Göran Nordlund (Finnish Meteorological Institute) for their interest and support throughout this work. Our thanks are also due to Dr. David Webber and Dr. David Martin (Safety and Reliability Directorate, United Kingdom) for their useful comments and cooperation.

Part of the work presented here was done with the financial support for the project 'Science and Technology for Environmental Protection, Research on the Dispersion of Two-phase Flashing Releases' (STEP-FLADIS) of the Commission of the European Communities. The funding of the Technical Inspection Centre, the Ministry of Environment and Neste Co. is acknowledged. We would also like to thank Mr Robin King for linguistic assistance with the manuscript.

Notation

A	area of cross-section (m^2)
C	drag coefficient (—)
D	aerodynamic drag force (N)
F	friction force (N)
$F_{g\text{-}b}$	gravity minus buoyancy force (N)
g	acceleration due to gravity (m/s^2)
h	height of the gas cloud (m)
k	Von Karman constant (—)
L	length scale (m)
m	mass (kg)
R	radius of the gas cloud (m)
Re	Reynolds number (—)
u, U	wind velocity (m/s)
u_{av}	average wind velocity (m/s)
u_*	friction velocity (m/s)
v	cloud speed (m/s)

z	height above the ground level (m)
z_0	roughness level (m)

Greek

δ	density (kg/m^3)
μ	dynamic viscosity (kg/(ms))
τ	turbulent shear stress (N/m^2)
θ	inclination angle of the slope (degrees)
ϕ	orientation angle of the slope (degrees)

Subscripts

a	ambient air
av	average value
c	gas cloud
e	edge of the gas cloud
g	released substance (gas)
$g-b$	gravity minus buoyancy
s	slope
t	top of the gas cloud
x,y	coordinates

References

1 R.E. Britter, Experiments on Some Effects of Obstacles on Dense-gas Dispersion, SRD R 407, Safety and Reliability Directorate, Warrington, Culcheth, 1989, 32 pp and appendix.

2 D.J. Hall, V. Kukadia, S.L. Upton, G.A. Marsland and M.A. Emmott, Repeat Variability in Instantaneously Released Heavy Gas Clouds Dispersing over Fences–Some Wind Tunnel Model Experiments, LR 805 (PA), Warren Spring Laboratory, Stevenage, 1991, 18 pp. and appendix.

3 P.W.M. Brighton, S.J. Jones and T. Wren, The Effects of Natural and Man-made Obstacles on Heavy Gas Dispersion. Part I: Review of earlier data, SRD/CEC/22938/01 AEA Technology, Safety and Reliability Directorate, Culcheth, 1991.

4 P.W.M. Brighton, Heavy-gas dispersion from sources inside buildings or in their wakes, I. Chem. E. Symposium on "Refinement of Estimates of the Consequences of Heavy Toxic Vapour Releases", UMIST, Manchester, 8 January 1986.

5 L.S. Fryer and G.D. Kaiser, DENZ: A Computer Program for the Calculation of the Dispersion of Dense Toxic or Explosive Gases in the Atmosphere, SRD R 229, UKAEA, Safety and Reliability Directorate, Warrington, 1979, 40 pp.

6 S.F. Jagger, 1983. Development of CRUNCH: A Dispersion Model for Continuous Releases of a Denser-than-air Vapour into the Atmosphere, SRD R 229, UKAEA, Safety and Reliability Directorate, Warrington, Culcheth, 1983, 26 pp.

7 C.J. Wheatley, A.J. Prince and P.W.M. Brighton, Comparison between Data from the Thorney Island Heavy Gas Trials and Predictions of Simple Dispersion Models, SRD R 1986, 355, UKAEA, Safety and Reliability Directorate, Warrington, Culcheth, 29 pp.

8 S. Hartwig, Open and controversial topics in heavy gas dispersion and related risk assessment problems, in: S. Hartwig (Ed.), Heavy Gas and Risk Assessment-II. D. Reidel, Dordrecht, 1983, pp. 1–25.
9 J.J. Stoker, Water Waves, Interscience, New York, NY, 1957, 567 pp.
10 S.J. Jones, D. Martin, D.M. Webber and T. Wren, The Effects of Natural and Man-made Obstacles on Heavy Gas Dispersion. Part II: Dense gas dispersion over complex terrain, SRD/CEC/22938/02, UKAEA Technology, Safety and Reliability Directorate, Culcheth, 1991, 57 pp.
11 C.I. Bradley, R.J. Carpenter, P.J. Waite, C.G. Ramsay and M.A. English, Recent development of a simple box-type model for dense vapour cloud dispersion, in: S. Hartwig (Ed.), Heavy Gas and Risk Assessment-II. D. Reidel, Dordrecht, 1983, pp. 77–89.
12 N. de Nevers, Spread and down-slope flow of negatively buoyant clouds, Atmos. Environ., 18(10) 1984) 2023–2027.
13 D.M. Deaves and R.C. Hall, The effects of sloping terrain on dense gas dispersion, J. Loss Prev. Process Ind., 3 (1990) 142–145.
14 J. McQuaid and B. Roebuck, Large Scale Field Trials on Dense Vapor Dispersion, Final Report to Sponsors on the Heavy Gas Dispersion Trials at Thorney Island 1982–1984, Report EUR 10029, Commission of the European Communities, Brussels, 1985, pp. 417.
15 J. McQuaid (Ed.), Heavy Gas Dispersion Trials at Thorney Island. Chemical Engineering Monographs, Vol. 22. Elsevier, Amsterdam, 1985, 435 pp.
16 J. McQuaid (Ed.), Heavy gas dispersion trials at Thorney Island-2, J. Hazardous Materials 16 Special Issue (1987) 501 pp.
17 J. Nikmo and J. Kukkonen, Modelling Heavy Gas Cloud Transport in Sloping Terrain, Report 2-91, Technical Inspection Centre of Finland, Helsinki, 1991, 44 pp.
18 G.K. Batchelor, Fluid Dynamics, Cambridge University Press, Cambridge, 1988, 615 pp.
19 W.F. Hughes and J.A. Brighton, Theory and Problems of Fluid Dynamics, Schaum's Outline Series in Engineering, McGraw-Hill, New York, NY, 1967, 265 pp.
20 B.Y. Underwood, Dry Deposition to Vegetated Surfaces: Parametric Dependencies, SRD R 442, UKAEA, Safety and Reliability Directorate, Culcheth, 1987, 51 pp.
21 A.J. Prince, D.M. Webber and P.W.M. Brighton, Thorney Island Heavy Gas Dispersion Trials–Determination of Path and Area of Cloud from Photographs, SRD R 318, UKAEA, Safety and Reliability Directorate, Culcheth, 1985, 13 pp.
22 NAG Workstation Library Handbook 1, NAG Ltd, Wilkinson House, Jordan Hill Road, Oxford, OX2 8DR, 1990.
23 W. Blumen (Ed.), Atmospheric Processes over Complex Terrain, Meteorological Monographs, vol. 23, number 45, Boston, MA, 1190, 323 pp.
24 R. Picknett, Dispersion of dense gas puffs released in the atmosphere at ground level, Atmos. Environ., 15 (1981) 509–525.
25 R.E. Britter and W.H. Snyder, 1988. Fluid modeling of dense gas dispersion over a ramp, J. Hazardous Materials, 18 (1988) 37–67.